

We are IntechOpen, the world's leading publisher of Open Access books Built by scientists, for scientists

6,900

Open access books available

186,000

International authors and editors

200M

Downloads

Our authors are among the

154

Countries delivered to

TOP 1%

most cited scientists

12.2%

Contributors from top 500 universities



WEB OF SCIENCE™

Selection of our books indexed in the Book Citation Index
in Web of Science™ Core Collection (BKCI)

Interested in publishing with us?
Contact book.department@intechopen.com

Numbers displayed above are based on latest data collected.
For more information visit www.intechopen.com



Colloidal Nanocrystal-Based Electrocatalysts for Combating Environmental Problems and Energy Crisis

Roshan Nazir, Abhay Prasad, Ashish Parihar, Mohammed S. Alqahtani and Rabbani Syed

Abstract

The serious threat that human beings face in near future will be shortage of fossil fuel reserves and abrupt changes in global climate. To prepare for these serious concerns, raised due to climate change and shortage of fuels, conversion of excessive atmospheric CO₂ into valuable chemicals and fuels and production of hydrogen from water splitting is seen most promising solutions to combat the rising CO₂ levels and energy crises. Among the various techniques that have been employed electrocatalytic conversion of CO₂ into fuels and hydrogen production from water has gained tremendous interest. Hydrogen is a zero carbon-emitting fuel, can be an alternative to traditional fossil fuels. Therefore, researchers working in these areas are constantly trying to find new electrocatalysts that can be applied on a real scale to deal with environmental issues. Recently, colloidal nanocrystals (C-NCs)-based electrocatalysts have gained tremendous attention due to their superior catalytic selectivity/activity and durability compared to existing bulk electrodes. In this chapter, the authors discuss the colloidal synthesis of NCs and the effect of their physiochemical properties such as shape, size and chemical composition on the electrocatalytic performance and durability towards electrocatalytic H₂ evolution reaction (EH₂ER) and electrocatalytic CO₂ reduction reactions (ECO₂RR). The last portion of this chapter presents a brief perspective of the challenges ahead.

Keywords: colloidal nanocrystals, electrocatalysis, size control, shape control, CO₂ reduction reactions, H₂ evolution reaction

1. Introduction

A clean environment and sustained energy resources are essential for future generations. With growing concerns for both dwindling traditional fossil fuels and global warming, there is an urgent need to develop renewable and environmentally benign alternatives to address these issues of mankind [1–3]. Currently, humans are mainly dependent on fossil fuels and thus extract carbon from the geosphere and put it into the atmosphere where it causes global warming. There are two methods that can be helpful in preventing and reducing carbon emissions. The first and

convenient way to stop carbon emissions is to move towards zero carbon-emitting resources. In view of this, hydrogen (H_2) produced by photo/electrocatalytic water splitting has shown great potential to become the fuel of the future. The merits have been attributed to its high energy density and it produces only one by-product of water upon combustion [4]. Thus H_2 , which is a zero carbon-emitting fuel, can be a promising solution to the mitigation of climate change. The second method is to capture carbon from the atmosphere and then store it back into the geosphere. However, the geosphere sequestration of CO_2 has no financial benefits. In contrast, chemical transformation of excess accumulated CO_2 from air into valuable industrial products, such as fuels (methanol, ethanol), hydrocarbon (methane, ethylene) and chemicals (formic acid, acetic acid), is an effective way to solve both global warming and energy crises [5, 6]. Furthermore, it has economic significance from an industrial point of view. However, carbon-di-oxide reduction (CO_2R) is a highly cumbersome and non-specific process. So far, several approaches, such as biochemical, chemical, thermal, photochemical and electrochemical catalysts have been explored to achieve aspirated activity and selectivity in this region [7–9]. Nonetheless, unlike other catalytic system electrocatalysts have gained tremendous attention due to its easy operation at ambient temperature and pressure. In addition, the selectivity of the product can be obtained by just adjusting reaction conditions, such as redox potential, electrode, and electrolyte, pH temperature and so on. The main advantage of using electrocatalysts is that they can be powered by renewable energy sources that emit zero carbon. For all these reasons, many research activities have shifted to the areas of EH_2ER and ECO_2RR (Figure 1) [10].

Over the years of time metal, metal oxide, metal sulphide have shown great promise in ECO_2RR and EH_2ER using electrocatalysis phenomenon. These electrocatalysts are being considered as a promising system that would be able to operate on a real scale without polluting environment. Whereas, there are still many limitations that are associated with electrocatalysts, such as high cost, poor product selectivity, high overpotential and low stability [11]. Colloidal Nanocrystal (C-NC) based electrocatalysts have become indispensable to overcome these limitations to certain extent owing to their larger surface to volume ratio, precise shape, long-term durability, and the plethora of configurations [12, 13]. These factors are important in influencing their efficiency, selectivity, and durability for EH_2ER and ECO_2RR . For example, variation in the size and/or shape causes alteration in reactivity at

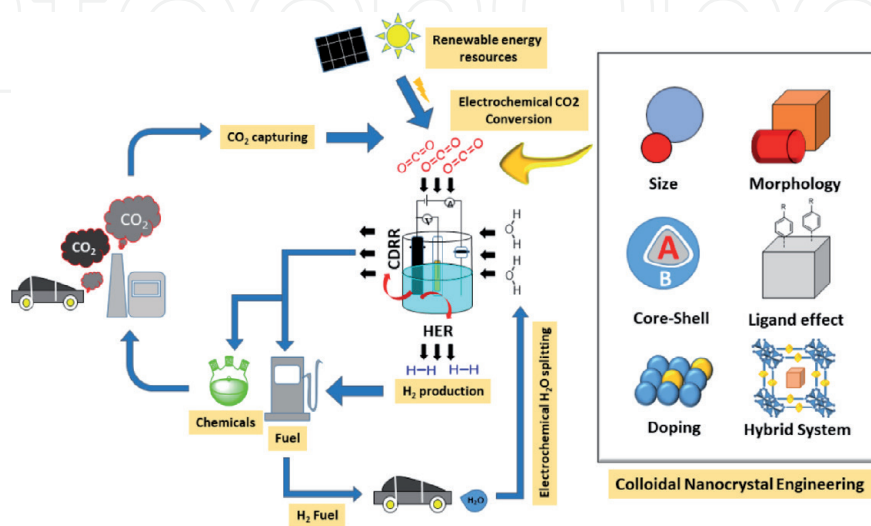


Figure 1. Electrochemical CO_2 conversion into fuel and H_2 production by using colloidal nanocrystal-based electrocatalysts.

different locations (edges/corners/faces) of the C-NC due to changes in a specific atomic-arrangement of active centers and crystal surface energy. The impact of these features will be discussed in detail as this chapter unfolds.

The purpose of this chapter is to elaborate on recent research developments and challenges in the field of heterogeneous C-NCs-based electrocatalysts for ECO_2RR and EH_2ER . In the first part of this chapter, colloidal synthesis of nanocrystals will be discussed. The second part of this chapter will address the structural aspects, such as size, shape, and composition, are important in tuning the catalytic efficiency, selectivity, and durability of NC-based catalysts for ECO_2RR . Here a brief introduction of effect of ligand functionalization and effect of MOF/NCs hybrid system on ECO_2RR activity will be also discussed. In the third part of this chapter, the role of C-NCs-based catalysts on EH_2ER , its activity and stability is given. Moreover, the detailed mechanism of EH_2ER is also discussed in this part. Finally, Authors have given extractive commentary that sheds light on the future perspective of ECO_2RR and EH_2ER in conclusion.

2. Colloidal synthesis of NCs

The C-NC is an inorganic material with a size of 1–100 nm and surface covering of protecting capping agents like polymer and surfactants molecules. Generally, the inorganic part exhibits characteristic features, such as optical, electrical, magnetic, and catalytic, that can be tuned by changing their physicochemical parameters, while surface capping guarantees the stabilization of these structures and paves the way for synthesizing more complex structures [14, 15]. The physical parameters like morphology and chemical composition of C-NCs can be easily adapted by varying their reaction parameters like monomer concentration forming inorganic core of NCs and judicious choice of capping substances for surface covering. Over the last two-three decades, researchers have gained good control over synthesis of high-quality and cost-effective NCs with uniform morphology and chemical constituents using colloidal synthesis [16–19]. The C-NCs approach has not only enhanced efficiency, selectivity of NCs, but also improved their service life. So far, researchers have found many commercial applications of C-NCs in various fields ranging from life sciences to the material world. One of the striking applications of C-NCs is in the field of biological imaging of cells, where quantum dots are used owing to their excellent fluorescent properties and also they do not photo-chemically bleach out like organic dyes [20]. Recently, quantum dots are being used commercially in LED displays also known as *QLED*-displays [21]. In addition, C-NCs-based photo/electro-catalysts for ECO_2RR and EH_2ER are being developed to solve the energy crisis and global warming. However, their uses at economical scale in this area is still facing challenges. Deep insights of C-NCs synthesis and the effect of C-NCs physicochemical parameters on their electrocatalytic properties need to be investigated for their successful applications at the economical level.

In general, C-NCs can be synthesized in both water and organic solvents. However, synthesizing a broad spectrum of NCs requires different reaction conditions that are much more feasible to achieve in organic solvents compared to water that is mainly used in the synthesis of noble metal C-NCs [14]. Therefore, in this section, authors will focus on organic phase C-NCs synthesis. Generally, C-NCs synthesis requires three major elements: 1) precursor molecules or building blocks forming inorganic core of NCs, 2) capping agents, and 3) organic solvents. Capping agents sometime act as solvent. The process of nanocrystal formation starts with transformation of precursor molecules into unstable and reactive species or monomers that usually occurs at quite high temperature. Thereafter, these monomers

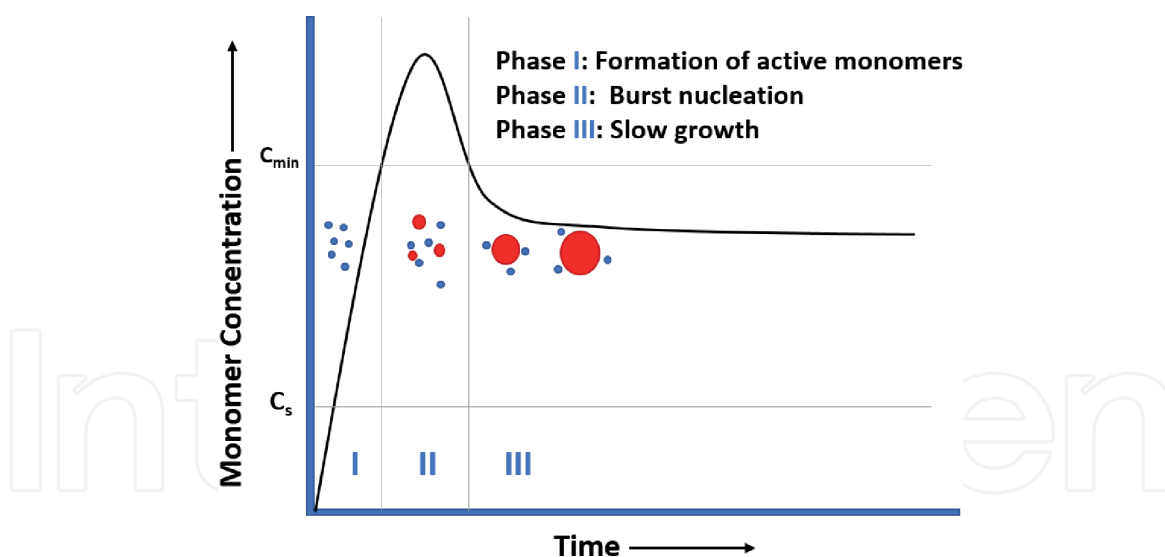


Figure 2. The LaMer mechanism based formation of active monomers, burst nucleation, and subsequent slow growth of colloidal nanocrystals. Adapted from [23].

lead to formation of C-NCs whose growth is mainly influenced by capping agents. The crystallization of C-NCs can be best understood using widely accepted LaMer mechanism as depicted in **Figure 2** [22–25]. Based on this mechanism, NCs development considered to have three major steps. In the first phase, the precursor molecules are converted to the reactive species, or monomer, and then eventually reach to a supersaturated phase (I), where no particle or second phase is still visible. In the next step, reactive species concentrate to the critical limit of supersaturation (phase II), at which a thermodynamically feasible state (**C_{min}**) is developed for nucleation, followed by monomers to form initial seed for nucleation. In the second phase, the supersaturation again drops at some point due to instant nucleation, reducing the monomer concentration below **C_{min}** that triggers the third phase (III) of the mechanism, that is, the growth of NCs. In this phase, because of monomer concentrations remain below **C_{min}**, therefore, NCs grow without forming further nuclei until they attain an equilibrium state. During the growth phase of C-NCs, capping agents also play an important role in determining the final morphology of NCs. First and foremost, the capping agent should have a tendency to adsorb on the surface of the growing NCs.

Secondly, capping agents are required to bind in such a way that it can desorb and adsorb on the surface of growing NCs during growth process, making growing NCs surface accessible for reactive monomers, yet surface covering of capping agents, overall, stabilize NCs [14, 26].

2.1 Size control in C-NCs synthesis

During NC synthesis, control over size uniformity is a prominent feature of contemporary synthetic methods. The LaMer mechanism discussed earlier not only explains the formation of NCs, but is also an approach to synthesize C-NCs with narrow size distributions. The essential element of LaMer approach to synthesize uniform-sized C-NCs is to divide crystallization into two disparate events; nucleation and growth. As discussed previously, the nucleation occurs for short periods of time, also known as burst nucleation, triggering a different growth phase where all nuclei then grow at the same rate without generating extra nuclei. The formation of extra nuclei during the growth phase can cause differences in the size of C-NCs because the newly formed nuclei will lag behind the previously growing NCs in growth kinetics. The

several methods utilize LaMer mechanism to grow uniform size C-NCs [24, 27]. The first example is seed-mediated growth method where reaction medium is introduced pre-developed nuclei at low monomer concentration to inhibit secondary nucleation. Therefore, these pre-developed nuclei further grow up to the desired size of C-NCs without creating extra nuclei. However, in order to obtain narrow size distribution of NCs, it is still required to control growth phase as well. The second example is hot injection method where the reaction medium at high temperature is rapidly supplemented with the precursor or reducing reagents to create a state of supersaturation that triggers subsequent burst nucleation. The next example is the heating up method where reaction medium pre-treated with precursor, and capping agents is heated at high temperature to induce the LaMer crystallization. Due to the simplicity of this method it is often used to synthesize C-NCs at large scale [28–30].

2.2 Shape control in C-NCs synthesis

Unlike the bulk materials, the physiochemical properties of C-NCs are also strongly dependent on their shape. In this chapter, authors will further discuss how the shape of C-NCs can be adapted to improve the service life, selectivity and efficiency of electrocatalysts. Generally, C-NCs shapes can be tuned by means of both thermodynamic and kinetic controls. In C-NCs synthesis, capping agents are used, primarily, to obtain the desired shape using their specific binding nature on the surface of the growing NCs [31]. If the surface adsorption of capping agents causes the decrement in surface energy of any specific facet, then the obtain shape will be favored by thermodynamically. Whereas, if capping agents serves an obstruction between growing NCs and diffusing monomers then the resulting shape of C-NCs will be governed by kinetic factors [32, 33]. Thermodynamically, the growing NCs attain it most likely shape by reducing its total surface free energy. For example, during the formation of fcc NC, the capping agents first selectively adheres to the (100) plans, which in turn, decreases their surface free energy [32]. These selective adsorptions onto the (100) plans causes transformation of cuboctahedron into cubic structure due the subsequent growth of higher energy facets. Whereas, in the kinetic regime, capping agents selectively adhere to some specific facets to lower their growth rate compare to others, resulting in various NCs shapes. Simultaneously, capping agents inhibit the diffusion of pre-deposited atoms over the NCs surface. In the real situation, however, the final shape of C-NCs is governed by the comparable kinetics of diffusion and deposition of monomers to growing NCs [32].

3. C-NCs-based catalysts for ECO₂RR

3.1 Mechanistic insight of ECO₂RR

Thermodynamically, CO₂ is a quite stable molecule (bond dissociation enthalpy of C=O is ~750 KJ mol⁻¹), so high energy is required for its activation. Moreover, the highest oxidation state of CO₂, causes problems for its selective reduction [34]. A catalyst in this regard is an alternative that offers reactive sites for its selective and rapid transformations. In this chapter, the authors are focusing specially on NC-based electrocatalyst for ECO₂RR. Generally, ECO₂RR involves several proton/electron transfers processes that take place at the cathode (catalyst). This process is considered to have three major stages. First, CO₂ is absorbed on the catalytic surface and its binding strength depends on the structure and composition of the NC as well as the nature of the electrolyte. Once it is absorbed, an electron is transferred

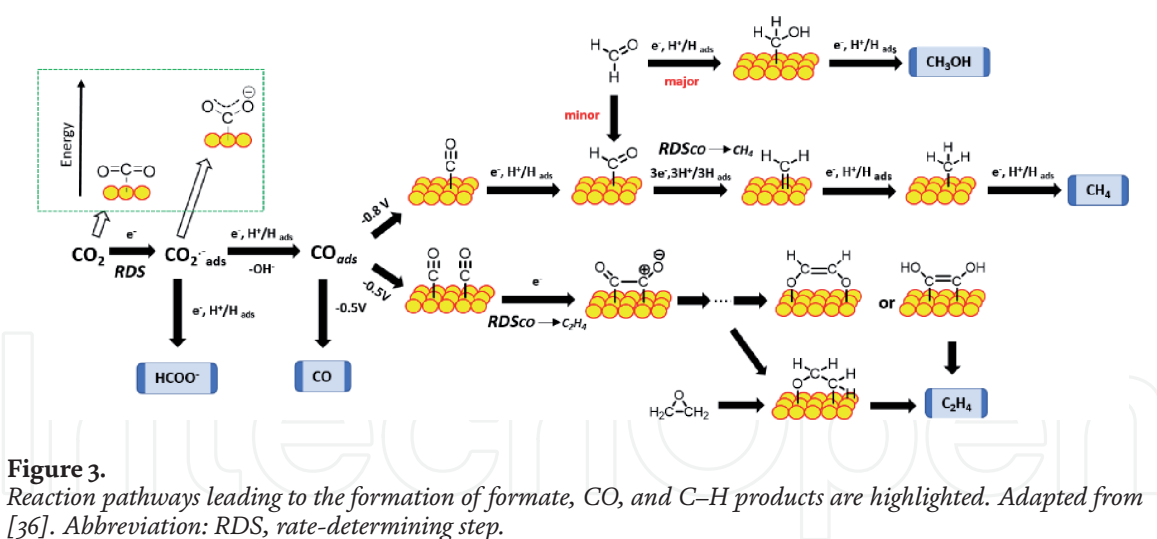


Figure 3.

Reaction pathways leading to the formation of formate, CO, and C–H products are highlighted. Adapted from [36]. Abbreviation: RDS, rate-determining step.

to the CO₂ molecule that produces surface bound CO₂⁻ Intermediate as depicted in **Figure 3**. This step is known as a rate-limiting step because it requires large reconstitution energy to convert linear CO₂ into twisted form, that is, CO₂⁻. For this reason, it requires extra potential (overpotential of –1.91 V) for electrochemical CO₂ conversion, even if it is thermodynamically feasible. After the formation of CO₂⁻ its reactivity on the catalytic surface determines resulting product in ECO₂RR. In principle, an optimal binding of the intermediate on the surface of the electrode is required for the rapid electron transfer process, thereby, increasing the selectivity and kinetics of the conversion. The reason for this is, a very strong affinity with intermediates will poison the surface of the electrode, while weak interaction will disrupt the electron transfer process. Sn, In and Pb, for example, represent weak interaction with CO₂⁻ intermediate, therefore, further reduction leads to production of HCOO⁻ as resulting product [35]. In comparison, CO₂⁻ on the surface of Ag, Au and Zn is reduced to COOH* which can be further reduced into CO* [35]. However, CO* has weak affinity towards these metal ions, and thus, gaseous CO is generated. Interestingly, Cu, which has been extensively studied by Hori et al., shows optimal binding with CO* and uniquely reduces CO₂ in many products including alcohol and hydrocarbons [35]. Whereas, metals, such as Pt and Ni, have a strong affinity for CO*, which prevents further reduction, and for this reason, these metals favor EH₂ER over ECO₂RR [35]. Therefore, optimal interaction between metal-based electrodes and surface bound intermediates has a significant importance in product selection and/or reaction rate.

Furthermore, it was realized that surface properties of electrocatalyst, such as, surface area, roughness, composition, and morphological design have profound influence on efficiency, selectivity and durability of electrodes in electrochemical reactions [37–38]. It is a general understanding that the higher surface area provides good economy of the active center on the surface relative to the bulk, and thus, accelerates CO₂ reduction. Similarly, Cu shows optimal coordination with CO, however, changes in surface structure, such as roughness, may deviate from their normal behavior. For example, Jiang et al. showed that the high population of under-coordinated sites on the rough surface of the Cu leads to the formation of oxygen-containing compounds and hydrocarbons compared to CO due to enhanced interaction with CO* intermediates [38]. However, it is still challenging to adjust the optimal binding energy for intermediates to increase selectivity/reactivity towards ECO₂RR, because of the large number of intermediates and many possible intricate pathways involved. Until now, many bulk metal-based electrodes have been investigated from both a material and structural point of view; however,

they are still facing many hurdles, such as: 1) high overpotential of the existing electrodes, 2) obtaining a mixture of products due to poor product selection of the catalyst, 3) deactivation of metal-based electrodes in short periods, 4) high cost of metal-based electrodes such as Ag, Au, Pt etc. discourages their use economically, 5) slow kinetics, or low activity. Beside there is always a competitive reaction EH_2ER to the ECO_2RR based on the thermodynamics. Rapid electron transfer in first step of electrochemical CO_2 reduction may be an effective strategy to suppress EH_2ER , which, in turn, accelerates ECO_2RR . In **Table 1**, the authors have summarized electrochemical Eqs. (1–16) of CO_2R in some valuable products such as CH_4 , CH_3OH , HCOOH , etc., with their respective equilibrium potentials in aqueous medium (pH 6.8) at 1 atm. and 25°C with respect to standard hydrogen electrode (SHE) [39, 40]. The equilibrium potential of the ECO_2RR , as provided, corresponds to the equilibrium potential of the EH_2ER .

3.2 C-NCs-based heterogenous catalyst for ECO_2RR

Recent studies have shown that nanometer-sized (1–100 nm) electrocatalyst is not only capable of reducing overpotential, but also shows an improvement in current density for CO_2 conversion. Regardless of the metal, the electronic structure of the catalysts at nanoscale is a key player in determining their efficiency, selectivity and durability for ECO_2RR . Several electronic factors have been determined, such as finite size effects, and the location of the d band center that can tune the binding strength of intermediates, such as CO^* , CHO^* , etc., on the nanoparticle

Products	Thermodynamic half-cell equations	E(V)
Hydrogen	$2\text{H}^+ + 2\text{e}^- \rightarrow \text{H}_2$	0.000
C1		
Methane	$\text{CO}_2 + 8\text{H}^+ + 8\text{e}^- \rightarrow \text{CH}_4 + \text{H}_2\text{O}$	0.17
Carbon-mono oxide	$\text{CO}_2 + 2\text{H}^+ + 2\text{e}^- \rightarrow \text{CO} + \text{H}_2\text{O}$	-0.10
Methanol	$\text{CO}_2 + 6\text{H}^+ + 6\text{e}^- \rightarrow \text{CH}_3\text{OH} + \text{H}_2\text{O}$	0.03
Formic acid	$\text{CO}_2 + 2\text{H}^+ + 2\text{e}^- \rightarrow \text{HCOOH} + \text{H}_2\text{O}$	-0.02
C2		
Acetaldehyde	$2\text{CO}_2 + 10\text{H}^+ + 10\text{e}^- \rightarrow \text{CH}_3\text{CHO} + 3\text{H}_2\text{O}$	0.05
Acetate	$2\text{CO}_2 + 8\text{H}^+ + 8\text{e}^- \rightarrow \text{CH}_3\text{COOH} + 2\text{H}_2\text{O}$	-0.26
Ethanol	$2\text{CO}_2 + 12\text{H}^+ + 12\text{e}^- \rightarrow \text{C}_2\text{H}_5\text{OH} + 3\text{H}_2\text{O}$	0.09
Ethylene	$2\text{CO}_2 + 12\text{H}^+ + 12\text{e}^- \rightarrow \text{C}_2\text{H}_4 + 4\text{H}_2\text{O}$	0.08
Ethylene glycol	$2\text{CO}_2 + 10\text{H}^+ + 10\text{e}^- \rightarrow \text{C}_2\text{H}_6\text{O}_2 + 2\text{H}_2\text{O}$	0.20
Glyoxal	$2\text{CO}_2 + 6\text{H}^+ + 6\text{e}^- \rightarrow \text{C}_2\text{H}_2\text{O}_2 + 2\text{H}_2\text{O}$	-0.16
Glycoaldehyde	$2\text{CO}_2 + 8\text{H}^+ + 8\text{e}^- \rightarrow \text{C}_2\text{H}_4\text{O}_2 + 2\text{H}_2\text{O}$	-0.03
C3		
Acetone	$3\text{CO}_2 + 16\text{H}^+ + 16\text{e}^- \rightarrow \text{CH}_3\text{COCH}_3 + 5\text{H}_2\text{O}$	-0.14
Allyl alcohol	$3\text{CO}_2 + 16\text{H}^+ + 16\text{e}^- \rightarrow \text{C}_3\text{H}_6\text{O} + 5\text{H}_2\text{O}$	0.11
Propionaldehyde	$3\text{CO}_2 + 16\text{H}^+ + 16\text{e}^- \rightarrow \text{C}_3\text{H}_6\text{O} + 5\text{H}_2\text{O}$	0.14
1-Propanol	$3\text{CO}_2 + 18\text{H}^+ + 18\text{e}^- \rightarrow \text{C}_3\text{H}_7\text{OH} + 5\text{H}_2\text{O}$	0.21
Hydroxyacetone	$3\text{CO}_2 + 14\text{H}^+ + 14\text{e}^- \rightarrow \text{C}_3\text{H}_6\text{O}_2 + 4\text{H}_2\text{O}$	0.46
Oxygen	$\text{O}_2 + 4\text{H}^+ + 4\text{e}^- \rightarrow 2\text{H}_2\text{O}$	1.23

Table 1. Thermodynamic electrochemical half-cell equations of CO_2R products, along with their relative standard redox potential (vs SHE in volt), or E(V) at pH 6.8 [39, 40].

(NP) surface and thus, alter the reactivity of NP-based electrocatalysts [41–43]. In addition, the geometric effect is an important factor that is crucial in stabilizing the specific intermediate during the reduction process, which leads to an increase in selectivity [44, 45]. When using C-NC-based electrocatalysts, electronic and geometric factors can be adapted to increase selectivity, stability and activity using several approaches, such as size adjustment, shape modification, compositional control, surface functionalization and reaction conditions. As discussed earlier, the nucleation and growth process can be optimized by changing the reaction conditions (thermodynamic and kinetic of the reaction) to achieve the desired C-NCs with well-defined composition, and morphology. Therefore, C-NCs-based catalytic systems have been found to be highly promising to lead the catalytic field that can achieve higher selectivity and efficiency than existing systems. Here, our focus will be mainly on to understand how properties like size, shape, morphology, composition and surface functionalization of nanocrystal affect efficiency and durability of C-NCs-based electrocatalysts for ECO₂RR.

3.3 Effect of C-NCs size on ECO₂RR

The size is an important factor for C-NC-based electrocatalysis because different size of C-NCs show different activity/selectivity towards ECO₂RR. Several studies have shown that alteration in size at nanoscale can affect both atomic distributions at various reaction sites (plans, edges, corners) and electronic structure of NCs, changing their catalytic characteristics. Therefore, the search for the optimal size C-NC showing the best efficiency, selectivity and durability requires contemporary research in this area. So far, to explore the effect of size towards ECO₂RR, different sizes of electrocatalysts have been evaluated, however, our focus here is towards C-NC-based electrocatalysts. Colloidal synthesis of NCs is an excellent approach to study different sizes of NCs while keeping other factors such as shape and composition stable. Loiudice et al. synthesized spherical and cubical Cu C-NCs in the size range of 7.5–27 nm and 24–63 nm respectively for ECO₂RR [46]. Their study has revealed unprecedented correlation between size of NCs and their electrochemical activity as well as selectivity for ECO₂RR. The activity of Cu C-NCs increases as size of NCs within same morphology decreases, however, this does not hold while comparing cubical NCs with spherical. For example, the 44 nm cube has higher current density than 27 nm sphere. To understand this phenomenon, the propensity of Cu (100) facet towards ethylene production can provide a better understanding. Based on previous findings, it is widely accepted that the Cu (100) plane is selective for the electrochemical reduction of CO₂ in ethylene. Additionally, edges in ethylene production are thought to be responsible for the absorption and stabilization of an important intermediate (i.e., COOH^{*}) as well as inhibiting EH₂ER. In this study, the X-ray diffraction pattern has shown a higher contribution of the Cu (100) plane in the nanocube than in the nanosphere and Cu foil. Interestingly, among all Cu C-NCs, a size of 44 nm exhibited highest selectivity with 50% FE for ethylene and overall 80% for ECO₂RR over EH₂ER. This can be ascribed to changes in atomic configuration at different sites of C-NC due to differences in size. As nanocube move from smaller to larger sizes, the number of atoms at the edges and corners decreases, however, the number of atoms at the plane site increases. As a result, it came close to the morphology of a single crystal, where all the atoms of the surface are populated on the (100) plane. And, as previously stated edges also play an important role in electrochemical reduction of CO₂ into C₂ products. Therefore, an optimal balance between ratio of edge to plane site in 44 nm Cu C-NC, suggesting not only its unique selectivity for C₂H₄, but also an overall activity towards ECO₂RR.

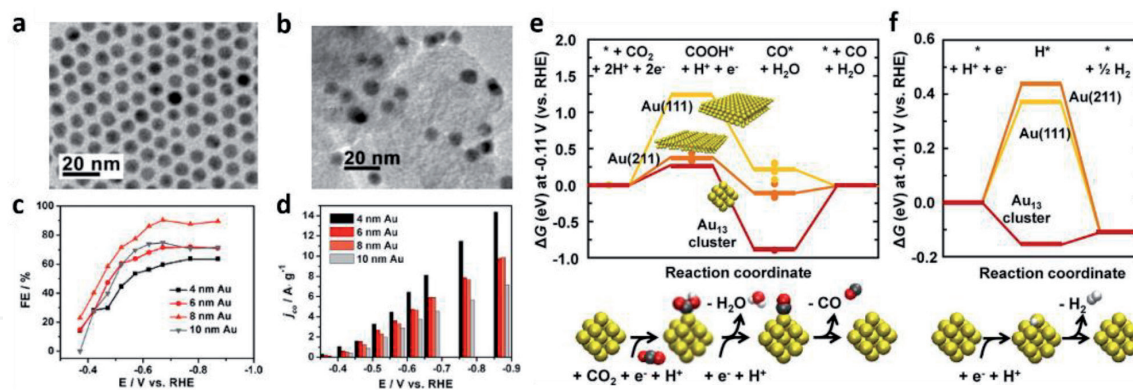


Figure 4. TEM images of (a) the 8 nm Au NPs and (b) the C-Au NCs. (c) Potential-dependent FEs of the C-Au on electrocatalytic reduction of CO₂ to CO. (d) Current densities for CO formation (mass activities) on the C-Au at various potentials. Free energy diagrams for electrochemical reduction of (e) CO₂ to CO and (f) protons to hydrogen on Au(111) (yellow symbols), Au(211) (orange symbols), or a 13-atom Au cluster (red symbols) at -0.11 V. reprinted with the permission from [47]. Copyright © 2013, American Chemical Society.

Similarly, Zhu et al. investigated the non-monotonic size-dependent selectivity of Au C-NCs for CO₂ reduction into CO [47]. Among Au C-NCs of size 4, 6, 8, 10 nm synthesized, the 8 nm exhibited a highest selectivity for CO production with FE of ~90% at -0.67 V vs. RHE as shown in **Figure 4(c)**. Based on the DFT calculations, the group concludes that dominance of edge sites at 8 nm C-NC facilitates selective CO₂ reduction in hydrocarbons, whereas depletion of corner sites inhibits EH₂ER. They have further reported the unique selectivity of Au₁₃ C-NC towards EH₂ER. Although Au₁₃ facilitates the formation of COOH* intermediate as compared to Au (211) and Au (111) facet, a stronger binding with CO* intermediate would lead to its lower tendency to produce CO₂ reduction products.

Additionally, as shown in **Figure 4(f)**, the free energy of formation ($\Delta G_{\text{formation}}$) of H* intermediates on Au₁₃ is lower than $\Delta G_{\text{formation}}$ of COOH*, suggesting the generation of H₂ at low overpotentials. Furthermore, this study is found to correspond to a size dependence study on the small size (2–15 nm) Cu C-NCs for ECO₂RR. For particle sizes at 5–15 nm, significantly higher activity and selectivity were found for H₂ and CO than for hydrocarbons. Moreover, particles smaller than 5 nm in size showed an exponential increase in the formation of H₂ and CO relative to hydrocarbons. This unique property of small C-NCs is due to an increase in under coordinated catalytic sites, which, in turn, strongly stabilize and bind with H* and CO* intermediates. Strong adsorption of H* and CO* intermediates is suggested to prevent subsequent hydrogenation of CO into hydrocarbons, so the increase in H₂ and CO production occurs at small (<5 nm) NCs.

3.4 Effect of C-NCs shape on ECO₂RR

The shape of the C-NC plays an important role in determining the selectivity/activity of the electrocatalysts. Several findings have shown that the shape-dependent C-NC activity/selectivity towards ECO₂RR is typically associated with the presence of specific crystal plane. For example, Suen et al. have revealed that cubic Cu C-NC (C-Cu) with mainly (100) facet shows enhanced selectivity towards C₂ products while octahedron Cu C-NC (O-Cu) with predominantly (111) facets shows selectivity for C₁ products in ECO₂RR [48].

Besides, Zhou et al. have illustrated the correlation between different shapes of C-NCs and their corresponding crystal planes using a stereographic triangle as depicted in **Figure 5(a)** [49]. The lower index surfaces, namely, the (100) (110) and (111) facets that lie on the three vertices of triangle, are present on the nanocrystal

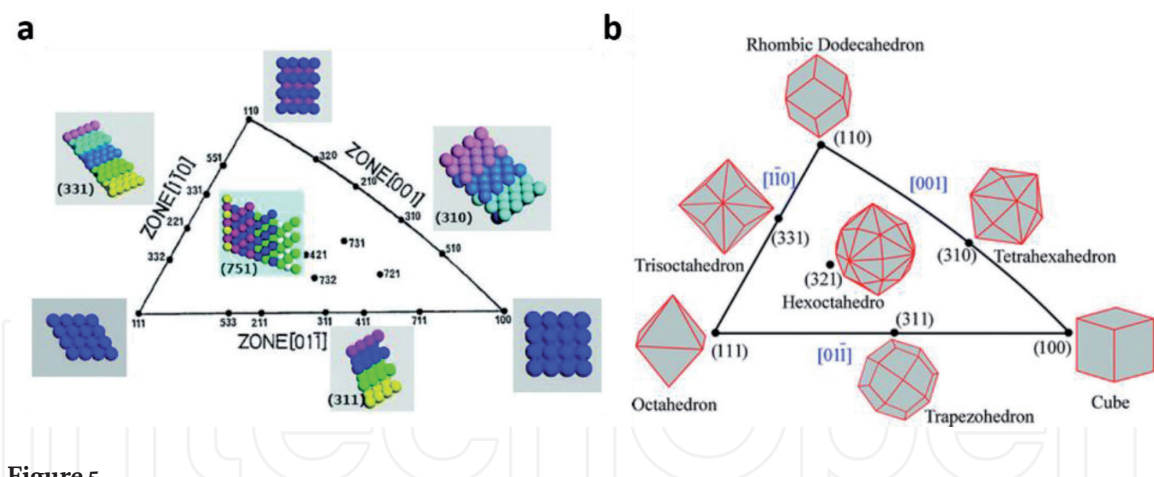


Figure 5. (a) Unit stereographic triangle of fcc single-crystal and models of surface atomic arrangement. (b) Unit stereographic triangle of polyhedral nanocrystals bounded by different crystal planes. Reproduced from [49] with permission from the Royal Society of Chemistry.

cube, octahedral, and rhombic dodecahedral, respectively. These low index surfaces are said to be less energetic, that is, catalytically less active. However, the plains lying on three sidelines of triangle and one which is residing inside the triangle are known as high index surfaces, that is, catalytically more active and stable. The high index planes (310), (311), (331), and (321) are correlated with tetrahedron, trapezohedron, trisoctahedron, and hexoctahedron, respectively, as illustrated in **Figure 5(b)**. The high energy of these polyhedron is attributed to predominance of atomic steps, islands and kinks on their surface. For example, a concave rhombic dodecahedron Au C-NC enclosed with multiple high index planes showed excellent activity and selectivity towards CO formation [50]. In addition, this particular structure of Au C-NC was found durable for longer period of time. Summing up, low coordinating high index planes with CN less than 7 exhibits high catalytic activity, selectivity, stability whereas low index planes with higher CN greater than 6 exhibits lower catalytic activity and stability.

Lattice strain has evolved as another factor that have a significant influence on electrocatalytic properties of C-NCs towards ECO_2RR . It was studied that strain generates a distortion in lattice, which, in turn, alters d-band center of metallic C-NCs. The altered d-band center either facilitates or lowers the adsorption of intermediates, as a result of that changing catalytic properties. Typically, upshifting of the d-band center facilitates adsorption of reaction intermediates on the surface of C-NCs. This is because, as the d band center approaches the Fermi level, which is the highest occupied state, the antibonding orbitals move over it, causing them to empty. This, as a result, strengthens the binding strength of the reaction intermediate on the catalytic surface and, therefore, enhances the reaction kinetics [51]

In general, lattice strain in C-NCs can be induced by shaping C-NC in various morphologies, which leads to the inward displacement of atoms at high-energy locations, such as corners and edges, while the outward displacement of atoms on planes to gain overall crystal stability. These compression and expansion in the atomic arrangement in the NCs induce aeolotropic strain gradients that may improve the catalytic efficiency/selectivity of C-NCs [45]. Octahedral and Icosahedron C-NC of Pd with similar sizes were examined by huang et al. to investigate the effect of strain on ECO_2RR . They observed that icosahedral/C C-NC shows higher FE (91% with -0.81 V vs. RHE) for CO production than octahedral/C C-NC in ECO_2RR . The molecular simulations and DFT calculations showed that surface strain in icosahedral C-NC enhanced catalytic selectivity due to shifting in d-band center, which, in turn, facilitates absorption of a key intermediate (COOH^*)

in ECO₂RR. Thus, surface strain in icosahedral C-NC boosts catalytic efficiency and selectivity for CO₂R [52].

3.5 Effect of C-NCs composition on ECO₂RR

The variation in composition of metal C-NCs is another intriguing factor that plays an important role in tuning electrocatalytic efficiency/selectivity towards ECO₂RR. Among other effects of composition, the synergistic effect where the mutual synergy between both electronic and geometric effects determines the activity/selectivity of C-NCs towards ECO₂RR is well known. The electronic effect can be understood by the concept of shifting in d-band center due to alteration in composition. In addition to the electronic effect, the geometrical effect also makes a significant contribution, where the particular atomic arrangement in the active center can modify the binding strength of the reaction intermediate, thereby improving the electrocatalytic efficiency/selectivity towards ECO₂RR [44]. Therefore, to understand the synergistic chemistry between geometric and electronic effects in this section, the electrocatalytic efficiency, selectivity and durability of bimetallic C-NCs and doped C-NCs electrocatalysts towards ECO₂RR will be discussed.

3.5.1 Bimetallic C-NCs

Until now, several bimetallic NCs have been investigated for ECO₂RR. For example, Kortlever et al. have found an optimal composition of a novel Pd₇₀Pt₃₀/C electrocatalyst highly active and selective towards HCOOH production. Moreover, this has a remarkably lower onset potential close to 0 V vs. RHE, making it best catalyst till the date [53]. However, usage of noble high-cost metals discourages its application on economical scale. Incorporation of non-noble metals such as Cu, Ni, Fe, etc., in bimetallic system could serve a better alternative to address high cost and stability of electrocatalyst. Kim et al. synthesized different composition of NCs including Au, AuCu, AuCu₃, Au₃Cu, and Cu, which were assembled in a monolayer on glassy carbon while keeping precise control over morphology (Size, Shape etc.) [44]. When considering electronic effect solely, pristine Au NC should have shown higher activity due to its optimal binding with COOH and CO intermediates. Interestingly, they have observed higher activity for Au₃Cu bimetallic C-NC than expected one. Therefore, electronic effect mere does not explain volcanic activity correlation for C-NCs. The geometric effect that works synergistically along with electronic effect ensure further stabilization of intermediates, thus, explaining optimal activity of Au₃Cu bimetallic C-NC towards electrochemical CO₂ reduction, among others. Previous studies have shown excellent properties of In based metal catalysts for selective CO₂ conversion into HCOOH. However, these metal catalysts suffer from limited current density and poor stability.

Kown et al. synthesized In₂O₃-ZnO C-NCs that showed excellent selectivity towards formation of HCOOH [54]. The XRD pattern showed that pre reduction of these C-NCs during electrolysis leads to the formation of In-Zn bimetallic C-NCs. Among all Zn_{1-x}In_x NCs, In_{0.05}Zn_{0.95} offered remarkable selectivity for HCOOH production at FE of 95% (-1.2 V vs. RHE) as well as with higher current density. The higher catalytic activity was seen in both Zn_{1-x}In_xO and Zn_{1-x}In_x with decreasing value of x. The XPS data has revealed predominance of O vacancies in bimetallic systems at lower x, which, in turn, decreases thickness of oxide layers in Zn_{1-x}In_x. Consequently, conductivity of Zn_{1-x}In_x C-NCs increases at lower x, therefore, facilitates rapid electron transfer processes in ECO₂RR. Thus, highest catalytic activity of Zn_{0.95}In_{0.05} C-NC is attributed to its remarkable conductivity. DFT calculations

revealed that tight binding of OCHO^* on pristine In, which impedes HCOOH production, has weakened by introduction of Zn in bimetallic C-NC. Therefore, mutual synergies of In with Zn in bimetallic system enhanced its catalytic selectivity in CDRR as compared to In [54]. Guo et al. have shown compositional effect in Cu_3Pt C-NCs is responsible for improved activity and selectivity for CH_4 [55]. It was observed that increasing Cu contents in bimetallic NC leads to desorption of more CO^* intermediates that subsequently gets protonated into CH_4 . Moreover, Pt which shows higher affinity for H^+ has significantly accelerated protonation of CO^* . However, higher Cu content beyond ratio of Cu and Pt (3:1) raised CO^* poisoning, and thus, declining in CH_4 production [55].

3.5.2 Doped C-NCs

In doped C-NCs, extrinsic or intrinsic introduction of impurities can cause a change in the electronic structure in a way that can enhance catalytic efficiency/selectivity and durability. For example, the incorporation of impurities can provide additional electrons (n-type) or additional vacancies (p-type), thereby, increasing the conductivity of the catalyst that would otherwise be poor in conductivity. Therefore, the increased conductivity may accelerate the electron transfer process in the ECO_2RR . Although many advances have been made in the field of doped C-NCs, some studies conducted in ECO_2RR . Recently, a group led by Kim et al. reported an unprecedented selectivity of vanadium ($_{23}\text{V}$) doped In_2O_3 C-NCs towards CH_3OH formation in addition to HCOOH and CO , previously not known with pristine In and In_2O_3 [56]. This can be understood using the commonly suggested scheme for producing CH_3OH shown in the **Figure 3**. The CO^* intermediate needs to be stabilized on the surface to proceed towards CH_3OH formation otherwise it may release as CO gas and terminate the reaction. The introduction of V^{3+} into In_2O_3 strengthens the binding of CO^* intermediate with NCs possibly due to the π -back donation from dopant to intermediate CO^* , and thus, reaction proceeds towards CH_3OH (FE of 15.8% at -0.83 V vs. RHS) [56].

3.6 C-NCs/metal organic framework hybrid

In the past years, molecular organic frameworks (MOFs) have received significant attention in the field of catalysis, including ECO_2RR , where they have been used primarily to provide solid support for molecular catalysts [57, 58]. The combination of MOF with C-NCs creates a class of hybrid materials that have demonstrated great potential to become future class of electrocatalysts with improved efficiency/selectivity and durability. Concerning this, a deep understanding of the material design and working principle of these novel hybrid systems is indispensable prior to implementing them practically. Recently, Guntern et al. investigated catalytic selectivity and durability of Ag C-NCs/Al PMOF hybrid system for electrochemical CO_2 reduction [59]. Based on UV visible and XPS data, it was concluded that electron transfer from MOF to Ag C-NC in this hybrid system increases electron density at Ag C-NC, thereby, facilitates electron transfer to CO_2^- intermediate. As in result, selectivity of Ag C-NCs/Al PMOF towards CO increases than pristine Ag C-NCs while decreases for H_2ER . Additionally, a small contribution of transport events due to diffusion of reactants and products within pores of MOF adds in the selectivity of NC/MOF hybrid towards CO . Besides, NC/MOF hybrid system showed better stability compared to bare Ag C-NCs at lower potential [59].

3.7 Ligand functionalized C-NCs

Capping agents such as, organic ligands, surfactants or polymers are engendering factors of surface anchoring molecules that are crucial in synthesis of C-NCs based catalysts with well-defined shape, uniform size distribution and different composition. After synthesis, these capping agents can significantly alter C-NCs catalytic efficiency in both positive and negative way by staying absorbed on their surface. For example, Wang et al. reported that catalytic activity of Ag NCs modified with capping agents increased by 53-fold compared to pristine Ag NCs towards CO_2RR [60]. In Several studies it has been shown that presence of surface molecule can affect active site of NC in numerous ways: 1) by perturbing electronic structure of active sites 2) by introducing steric hindrance that impedes diffusion of absorbates reaching at active center 3) by blocking selective facets of C-NCs, which, in turn, could enhance selectivity and activity. Moreover, chiral ligands can be used to produce stereoselective products. Therefore, surface functionalized NCs has opened a new window in the field of electrocatalytic reactions where unprecedented control over efficiency/selectivity can be achieved by ligand design [61, 62]. However, researchers still have a limited understanding of how these anchoring ligands affect the local electronic environment of NC and how the backbone of anchoring ligands regulates reactivity between NC and surrounding reactants, or reaction intermediates.

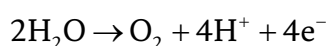
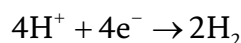
Pankhurst et al. have tuned CO_2RR selectivity of Ag C-NCs using different imidazolium ligands [63]. Here they were able to introduce different organic component by varying tail and anchoring groups on imidazole motif. When performed CO_2RR , the ligand bearing NO_2 anchoring group with octyl tail-found highly selective towards CO with FE of 92%. It was concluded that interaction between cationic imidazolium group with CO_2 increases population of this reactant over the catalytic surface. Furthermore, an optimal chain length of ligand tail-group increased hydrophobicity of surface, and thus, increases selectivity and efficiency for CO_2RR by inhibiting EH_2ER . However, electronic changes induced by ligand anchoring-group did not improve significantly properties of electrocatalyst. The next example of ligand surface functionalization for CO_2RR discusses N-heterocyclic-carbine functionalized Au C-NCs (Au C-NC-Cb) from group led by Cho et al. The significant downfield shifting in ^{13}C NMR peaks of NHC reveals strong electron donation from ligand to metal, making Au C-NCs surface electron-rich. As in result, it facilitates the electron transfer process to CO_2 , and thus, enhances efficiency of Au C-NC-Cb relative to bare Au C-NCs [64].

4. C-NCs-based heterogeneous catalyst for EH_2ER

The concept of using electric current to control various chemical reactions achieved much attention, since the time when humankind invented first power resources. Splitting of water to produce hydrogen and oxygen gas started much earlier, but now it has started at large scale in industrial process and seems to play a crucial role in combating the future energy crisis. The increasing demand for energy day by day and the shortage of fossil fuels have encouraged scientists to develop a renewable and clean source of energy.

Hydrogen is considered a clean source of energy because by-product of H_2 combustion is H_2O and the starting material to obtain H_2 is water, therefore, an efficient and clean source to supplant the depleting fossil fuels [65–67].

Moreover, H₂ produces highest energy on combustion of per unit mass relative to any other fuels, thus, leading to become a fuel of future. The H₂ can be produced by electrochemical water splitting reaction which is an endothermic process with a potential of $\Delta E^\circ = 1.23 \text{ V}$ and $\Delta G^\circ = 237.2 \text{ kJ mol}^{-1}$. Water splitting generates both hydrogen and oxygen. For the process of electrochemical water splitting the reactions that occur at anode are called as oxygen evolution reaction (O₂ER) and the reactions which occurs at cathode are called as H₂ evolution reaction (H₂ER) [68]. Electrocatalysis is actually an attempt to elucidate and predict observable phenomena like overall activity of the reactions that occur on the surface of electrode by the interactions of electrode/electrolyte interface. Development of an efficient electrocatalyst is important to minimize the energy losses during the electrocatalytic splitting of water to produce hydrogen and oxygen gas. **Figure 6** shows a diagrammatic representation of evolution of hydrogen (Depicted to the left-side of **Figure 6**) and oxygen (depicted to the right side of **Figure 6**) gas on the surface of glassy carbon electrode (GCE) after deposition of catalyst on its surface.



The reactions which are central to hydrogen energy are two types. These are hydrogen evolution ($2\text{H}^+ + 2\text{e}^- \rightarrow \text{H}_2$) and hydrogen oxidation ($\text{H}_2 \rightarrow 2\text{H}^+ + 2\text{e}^-$) reactions. The research of oxidizing and evolving hydrogen was started in 1960 but it gained importance in 1970 and 1990 when the shortage of oil was realized [69]. The most success in this regard was achieved when precious metals like platinum (Pt) were used. Metal NPs on the surface of carbon also showed great success in H₂ER and hydrogen oxidation reaction (H₂OR).

In the world of EH₂ER electrochemistry, recent merge of computational quantum chemistry and nanotechnology have shown great progress in explaining

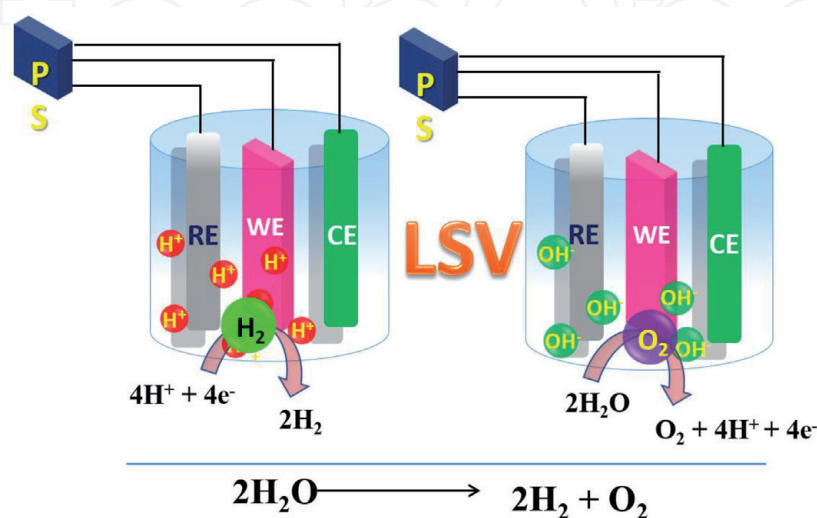


Figure 6.

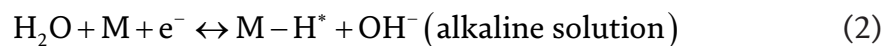
Diagrammatic representation of formation of hydrogen during hydrogen evolution reaction and formation of oxygen during oxygen evolution reaction on the surface of glassy carbon electrode. Abbreviation: LSV - linear sweep voltammetry, WE - working electrode, RE - reference electrode, CE - counter electrode.

fundamentals and basics of EH_2ER with much emphasize on its utility and storage [51, 70, 71]. Metallic Pt is considered as ‘state of the art catalyst’ and exhibits small Tafel slope values and extremely high exchange current density (j_0) [72–74]. However, because of high cost and less availability of Pt, a sustainable, cost effective, and stable catalyst needs to be developed. So, there have been efforts to synthesize the EH_2ER active catalysts from the transition metals that are abundant in nature.

4.1 Mechanistic overview of EH_2ER

EH_2ER kinetics has a long history and have been explained in detail [69]. EH_2ER ($2\text{H}^+ + 2\text{e}^- \rightarrow \text{H}_2$) is a process involving a series of electrochemical steps which takes place on the electrode surface and results in the evolution of hydrogen. There are two mechanisms in acidic and basic conditions accepted universally as shown in **Figure 7** [75]. These steps are:

1. Electrochemical hydrogen adsorption (Volmer reaction) (Eq. (1), (2))



This step is followed by.

2. Electrochemical desorption (Heyrovsky reaction) (Eq. (3), (4))

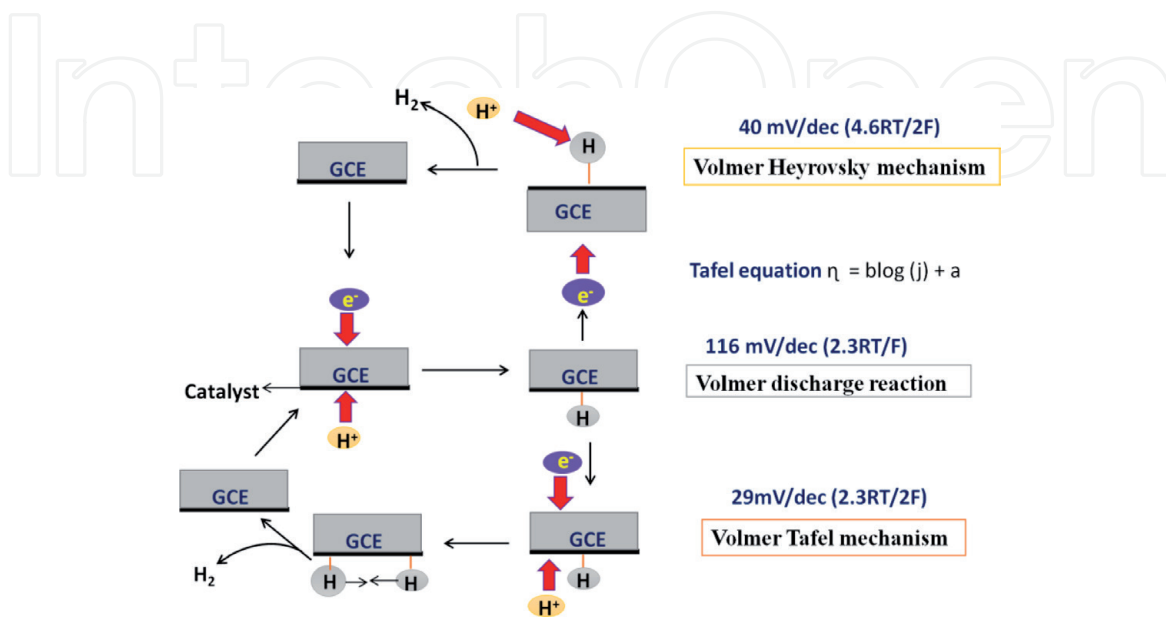
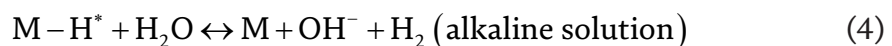
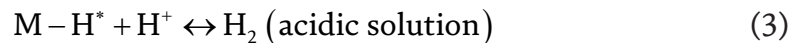
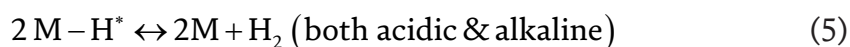


Figure 7. Mechanism of hydrogen evolution reaction on surface of glassy carbon electrode (GCE). Abbreviation: GCE - glassy carbon electrode.

Or,

3. Chemical desorption or combination reaction (Tafel reaction) (Eq. (5))



In the above reactions, H^* indicates an adsorbed hydrogen atom that has been adsorbed chemically on the surface of electrode (M) at the active site. These reaction pathways are highly dependent on electronic and chemical properties of the electrode surface [76]. Tilak et al., explained that rate controlling steps (1, 2 and 3) is predicted by deducing Tafel slope values from EH_2ER polarization curves [72]. The mechanism and rate determining step is studied by the Tafel slope. Tafel slope is an inherent and interesting property because it gives information about the potential difference required to increase or decrease the current density by 10-fold. Tafel slope is also useful to determine the effectiveness of a catalyst. In order to calculate the Tafel slope the linear portion of the Tafel plots is to be fitted in the Tafel equation ($\eta = b \log(j) + a$, where η = overpotential, b = Tafel slope, and j = current density) [77, 78]. Theoretical facts about Tafel slope have been derived from Butler-Volmer equation and it is proved for three limited cases. First, if the discharge reaction proceeds very quickly and H_2 is evolved by the rate determining combination reaction (Tafel step). The slope value is 29 mV dec⁻¹ at 25°C (2.3RT/2F). Second, if the discharge reaction proceeds very quickly and H_2 is evolved by the rate determining desorption reaction (Heyrovsky step). The slope value for this step is 40 mV dec⁻¹ at 25°C (4.6RT/3F). Third, if the discharge reaction proceeds very slowly and then the rate determining step will be Volmer step irrespective of the fact whether H_2 is evolved by the combination reaction or the desorption reaction. The Tafel slope is 116 mV dec⁻¹ at 25°C (4.6RT/F). The detailed mechanism is shown in **Figure 7**. It is evident that reaction (1) represents chemical adsorption, whereas, reaction (2) and (3) exhibits H atoms desorption from the electrode surface, which are competing with each other. Sabatier and co-workers came with an idea (Sabatier principle) that a better catalyst should not only form a strong bond with adsorbed H^* and facilitates the proton electron transfer process, but also it should be weak enough in facial bond breaking to assure quick release of H_2 gas [79]. It is difficult to establish a quantitative relationship between energies of H^* intermediate and rate of electrochemical reaction owing to absence of directly measured surface-intermediate bonding energy values [80]. However from the perspective of physical chemistry, both for H^* adsorption and H_2 evolution on the catalyst surface can be determined from the change in free energy of H^* adsorption (ΔGH^*) using EH_2ER free energy diagram [81]. According to Sabatier principle, under the condition $\Delta GH^* = 0$ will have maximum overall reaction rate (expressed in terms of EH_2ER exchange current density, j_0).

4.2 Metal-based C-NCs for EH_2ER

An important correlation between ΔGH^* and j_0 have been proposed in the form of “volcano curve” for a wide variety of electrode surfaces as illustrated in **Figure 8** [81, 82]. Pt group of metals are the most efficient in the process and that’s why are found at the top of the volcano curve, because they have small Tafel slope and quasi zero onset potential.

However, due to high cost of Pt, various research groups have been working on modifying Pt group metals such as engineering the NCs. Crystal plane (110) of Pt NCs has been proved good surface for EH_2ER . Like Pt, Palladium (Pd) NCs have

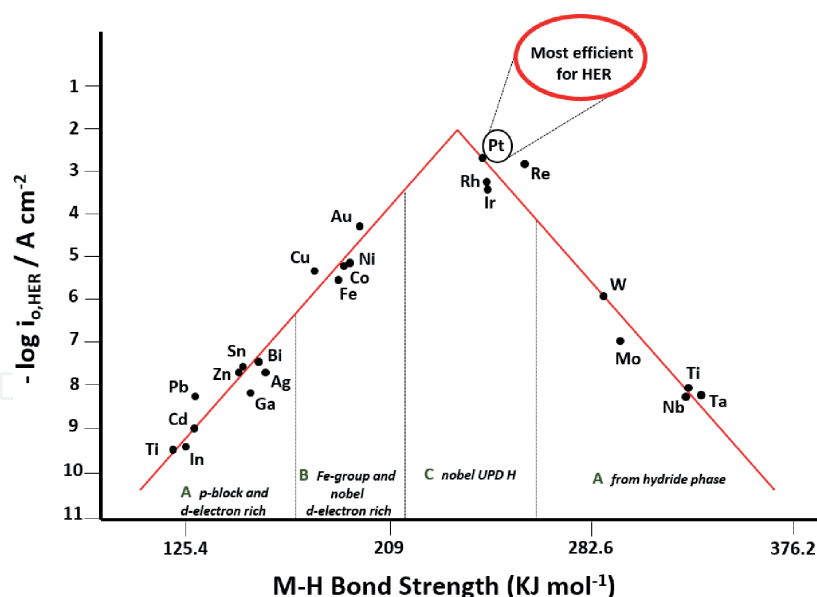


Figure 8.
 Volcano plot for $\log I_0$ values for HER as a function of M-H bond energy. Adapted from [83].

been showing great promise as it is in the same group and has almost same size and its lattice matches about 0.77% to Pt, good thing about Pd is that it is comparatively cheaper than Pt. Pd has one advantage that it can adsorb hydrogen from both electrolytes and the gas phase. Pd can be loaded on various supports to increase its activity as it alters surface area and electronic conductivity of the nanocrystals [84]. Huang et al. observed that Pd C-NCs deposited on carbon paper substrate has activity higher than Pt black electrode and it required very less catalyst loading that is $0.0106 \text{ mg cm}^{-2}$ [85]. One thing to be noted about Pd is that it has higher activity in acidic medium than alkaline medium because of lower Pd-H binding energy and lower activation energy, acid ($32.3 \pm 0.7 \text{ kJ/mol}$) and base ($38.9 \pm 3.0 \text{ kJ/mol}$). Ruthenium (Ru) NCs are also being explored for EH_2ER . As the Sabatier principle suggest that catalyst should not have much stronger binding to the hydrogen and should possess moderate binding capacity so desorption is easy, Ru-H follows this trend as it has $\sim 65 \text{ kcal/mol}$ energy for Ru-H bond and thus less activation barrier for desorption process [86]. Ru C-NCs are usually used with some support as they have durability problems because of aggregation. One such example where Joshi et al. used Ru C-NCs supported with Tungsten (W). DFT calculations suggest that Ru (0001) has high H_2 binding to surface energy but using W support, it could reduce the H_2 adsorption energy and changes the electronic environment thus making it similar to Pt (111) and increases its activity for EH_2ER process [86]. Baek et al. revealed that Ru when deposited on graphene nanoplatelets (GnP) to form Ru@GnP, its activity usually surpasses that of Pt/C in both acidic and alkaline medium. This happens because it is more stable, possess low Tafel slope (30 mV dec^{-1} in $0.5 \text{ M aq. H}_2\text{SO}_4$; and 28 mV dec^{-1} in 1.0 M aq. KOH) and also has comparatively low overpotential at 10 mA cm^{-2} (13 mV in $0.5 \text{ M aq. H}_2\text{SO}_4$; 22 mV in 1.0 M aq. KOH) [87]. Not only Pt, Pd, Ru, metals like Iridium (Ir) are also explored for the EH_2ER process and also earth abundant metals are used but they are prone to corrosion in the presence of alkaline and acidic medium. Thus, the other way is using non-noble metals for the process.

Non-Noble metals follow this trend for the catalytic activity Nickel (Ni) > Molybdenum (Mo) > Cobalt (Co) > W > Iron (Fe) > Copper (Cu) which is calculated using the voltammetric techniques [88]. Ni shows a very good catalytic activity when using in the hybrid form of Ni/NiO/CoSe₂ because this composite helps in less resistance to charge transfer. But this hybrid has poor

stability as Ni does not work well in acidic medium [89]. Recent studies by Qiu et al. found that when Ni is used with graphene it forms Ni-C bonds which increases the stability as well as the activity of the catalyst and is the best one proved for the process using Ni [90]. Co when embedded with Nitrogen rich CNTs forms a very good catalyst that catalyzed at all pH ranges. The reason for this good activity at all pH ranges is the N-doped content and the structural defect caused by the caused by pyrolysis of the Co-NRCNTs at higher temperatures [91]. These Nitrogen rich Co based catalyst can also be dispersed over the nanofibers for improving the catalytic activity. These particular catalysts also showed good stability for various potential cycles of process [92]. Along with Co and Ni Other Non-Noble metals are also used for the EH₂ER process including Fe, W, Mo but these all face the problem of their stability and there is still a lot to discover in this field.

4.3 Non-nobel metal-based C-NCs for EH₂ER

To avoid using precious noble metals there have been a plethora of reports using non-noble metal-based C-NCs for EH₂ER process. Some of them are transition Metal Oxides (TMOs), transition metal nitrides (TMNs), transition metal carbides (TMCs), transition metal borides (TMBs), transition metal phosphides (TMPs), transition metal dichalcogenides (TMDs). In this section the authors will discuss about the advancement in these types of NCs their advantage and disadvantages all. Although there are huge number of reports on transition metal-based compounds, but Mo and W display very good catalytic activity out of all of them. TMOs are easily available, stable, not harmful to the environment and obviously not precious like noble metals and thus is a good class of EH₂ER catalysts. Out of all the TMOs, Mo (MoO₂) and W (WO₂) based EH₂ER catalysts are best as they have high electrical conductivity as compared to other TMOs the credit goes to their monoclinic and distorted rutile crystal structure [93]. Compact MoO₂ faces have a problem of aggregation and thus various research groups tried to bring changes in the catalyst by decreasing the size of structure, forming hybrid composites, doping the MoO₂ or even introducing surface defects. One such example where Yu et al. encapsulated MoO₂ with phosphorous-doped porous carbon embedded on rGO to form MoO₂@PC-rGO which has a small tafel slope (41 mV dec⁻¹) and less over potential ($\eta_{10} = 64$ mV). Here electronic coupling between MoO₂ and rGO along with the porous carbon layer helps in getting rid of the problem of aggregation and improves its efficiency as a EH₂ER catalyst [94]. The other important metal oxide for EH₂ER is WO₂. Reports have revealed when WO₂ have vacancies of oxygen, it provides large number of active sites and thus augmented the EH₂ER process as compared to the compact WO₂ counterpart. One such example where Shen et al. encapsulated WO_x with Carbon on a Carbon support to form WO_x@C/C which has EH₂ER activity comparable to Pt metal with ultra-low overpotential ($\eta_{60} = 36$ mV) and very small tafel slope (19 mV dec⁻¹) which is because of the thick carbon shell helping in increase of charge transfer and also changes the Gibbs free energy values of H* for different adsorption sites [95].

TMNs are also other class of noble metal-compound based NCs for EH₂ER. The importance lies in the fact that they possess more contraction of the d bands and density of state near Fermi level because of interaction of negatively charged N atom which expands the lattice and increases it efficiency as a catalyst to make it comparable to noble metals like Pt, Pd [96]. As discussed earlier, whenever NCs are encapsulated with carbon material they tend to avoid aggregation and improve the efficiency as a catalyst. One such example where Shao et al. developed MoN

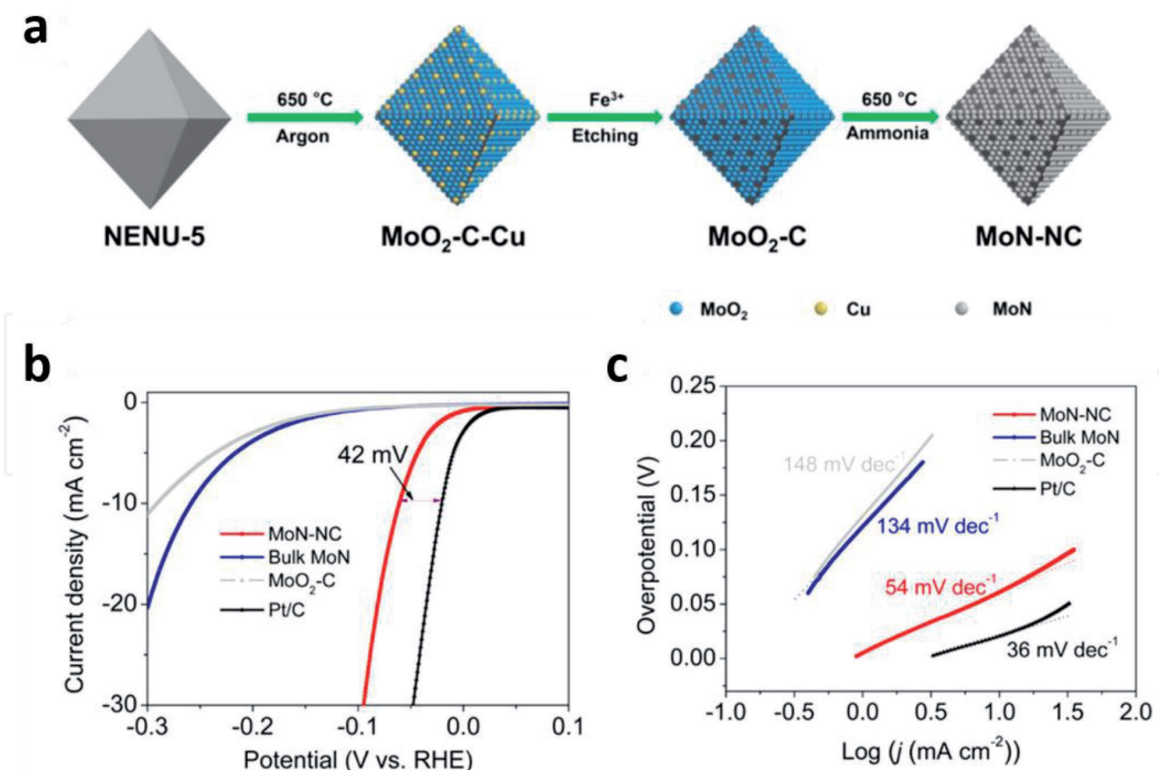


Figure 9. (a) Procedure for the synthesis of MoN-NC nano-octahedrons derived from Mo-based MOFs (b) polarization curves (*iR* compensated) in 0.5 M H₂SO₄ at a scan rate of 5 mV s⁻¹ and (c) the corresponding Tafel plots of the MoN-NC nano-octahedrons, intermediate MoO₂-C, bulk MoN, and 20% Pt/C catalysts. Reprinted with the permission from [97]. Copyright © 2017, American Chemical Society.

encapsulated with N-doped carbon material to form MoN@NC which exhibited very low overpotential ($\eta_{10} = 62 \text{ mV dec}^{-1}$) and small tafel slope (54 mV) as depicted in **Figure 9 (c)** [97]. WN also possess same features as they exhibit less activity when used as it is but when encapsulated with carbon material its activity increases, one such example is using WN encapsulated with N doped graphene material (WN_xNRPGC) which has high electrocatalytic activity because of the formed hetero-architecture [98]. Ni based TMNs have also been explored a lot as they possess high electrocatalytic activity.

4.4 Metal-alloy-based C-NCs for EH₂ER

Whenever there is introduction of another element in the lattice of the metal synergistic effect comes into effect (intercalation of crystal planes, change in the metal-metal length to have strain and also formation of heteroatom bond to give ligand effect). This result in the change of electronic properties and morphology and hence in the electrocatalytic activity of the catalyst. To reduce loading of noble metals they are doped either with other comparatively cheap noble metal or sometimes with transition metal. The authors will discuss examples of both these types. Pt can be doped with Pd to form 1-D single crystalline material (thickness 3 nm) which increases the Pt utilization efficiency this was done by Liu et al. using solution phase method directed by surfactant [99]. Pt can also be doped with non-noble metals one such example is the use of Pt-Co alloy encapsulated on carbon material, thus possessing high activity as displayed by the small tafel slope of 20 mV dec⁻¹. This catalyst requires very less loading of Pt (ca. 5 wt %) and has activity comparable to Pt/C catalyst [100]. Using the same strategy Pd and Ru can also be doped

with either noble metal or transition metals, some examples are Pd-Au catalyst, Pd-Co catalyst, Ru-Co and Ru-Ni [101–104].

Transition metal can be alloyed with transition metal itself and thus it can be a very good alternative for noble metal electrocatalysts because of the cost-effective nature of them. These alloys could either be binary alloys or ternary alloys, the authors will discuss examples from both binary and ternary alloys. Ni can form alloy with various other transition metal, but Ni-Mo binary alloy is considered best for the EH_2ER . Zhang et al. worked on the synthesis of MoNi_4 supported over the MoO_2 cuboids over the Ni foam. This catalyst has the activity similar to Pt/C with zero onset potential and $\eta_{10} = 15$ mV and very low tafel slope of 30 mV dec^{-1} [105]. Ni binary alloys face the problem of corrosion which can be overcome by using the carbon support along with the Ni based alloy. Co also form binary alloys with Fe using N-doped carbon-based support. Also, Co can be alloyed with Mo forming good electrochemical catalyst for EH_2ER such as Co_3Mo having an overpotential of $\eta_{10} = 68$ mV and tafel slope of 61 mV dec^{-1} [106]. Ternary alloys in the recent times have gained popularity for EH_2ER electrochemical catalysts as electronic and morphological features of catalyst can be tuned by variation in compositions of various metals and thus it can act as the good promising substitute for the noble-metal-based EH_2ER catalyst. One such example is the use of small amount of Pt (4.6%) to the Fe-Co binary alloy to form the PtCoFe@CN electrocatalyst which demonstrated activity similar to that of commercial 20% Pt/C having an overpotential of $\eta_{10} = 45$ mV as depicted in **Figure 10(b)** [107]. Research is still going on to prepare the ternary alloys without using the noble metals in it and that will really be the landmark in this field as it will be a catalyst with cost-effective nature.

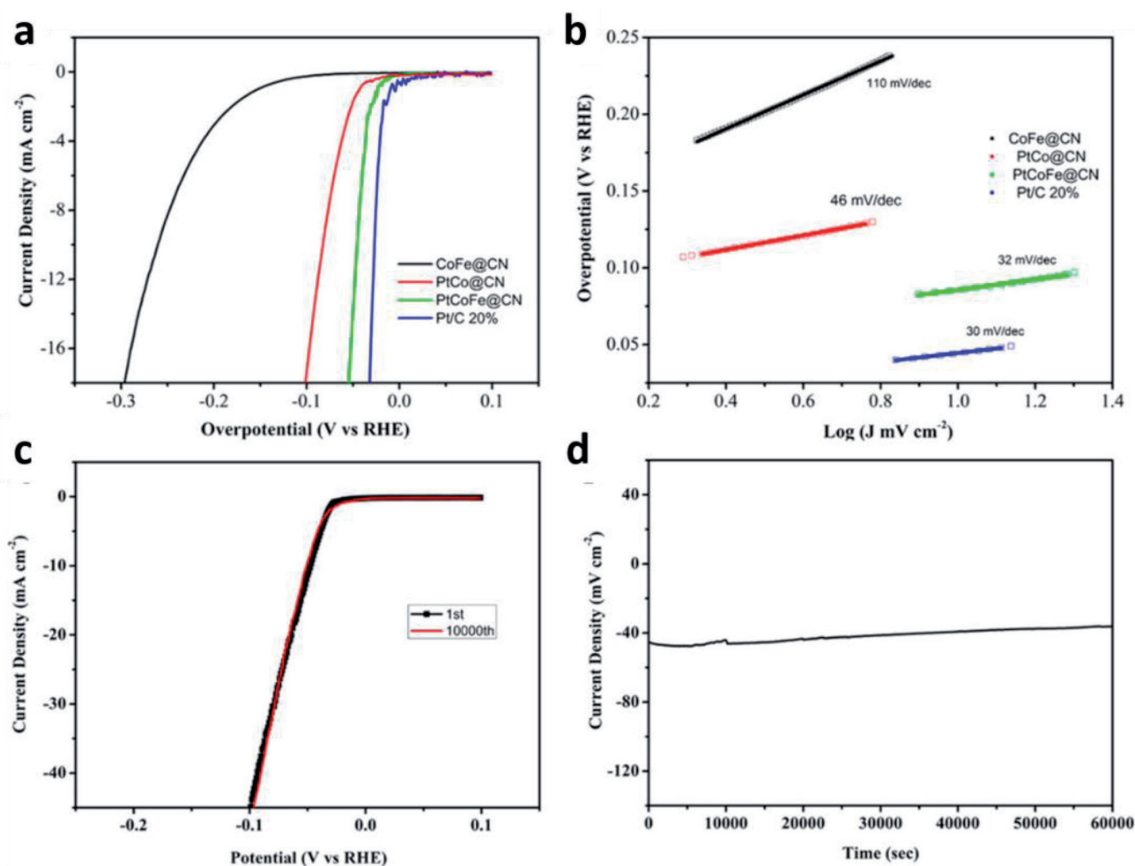


Figure 10.

(a) Polarization curves (b) Tafel plots of samples (c) polarization curves of PtCoFe@CN 1st and 10000th cycles (d) Amperometric *i-t* curves of PtCoFe@CN. Reprinted with the permission from [107]. Copyright © 2017, American Chemical Society.

5. Conclusions

This chapter discusses a thorough study of recent achievements by C-NCs-based electrocatalysts for ECO_2RR and EH_2ER . In this chapter, the authors have tried to summarize role of C-NCs in ECO_2RR and EH_2ER and the scope of these two important electrocatalytic reaction in combating the energy crises for human kind in introduction part. The examples that are discussed in this chapter were taken from recent reports in literature. The first part of this chapter sheds light on colloidal synthesis of nanocrystals. The second part of this chapter emphasizes on effect of shape, size and composition in determining the catalytic activity, selectivity and stability of C-NCs for ECO_2RR . Here the effect of ligand functionalization and MOF/NCs hybrid system on ECO_2RR activity is also illustrated. The third part of this chapter addresses the role of C-NCs-based electrocatalysts on EH_2ER , its activity and stability. In this part, indepth study about mechanism of EH_2ER is also discussed. Although a lot has been done in ECO_2RR but ECO_2RR still face a big challenge in selectivity, similarly in EH_2ER a lot of research has been dedicated to find a substitute of state-of-art Pt/C catalyst which is very much expensive. However, researchers have been successful in discovering the costeffective electrocatalysts which are as good as Pt/C but they are still facing the stability issues.

Author Contributions

RN, AP (Abhay Prasad), AP* (Ashish Parihar) designed the study, reviewed the literature, wrote and edited the manuscript. MSA and RS provided the inputs while editing the manuscript. The complete review article was edited and finalized by RN, AP, and AP*.

IntechOpen

IntechOpen

Author details

Roshan Nazir^{1,2*}, Abhay Prasad³, Ashish Parihar⁴, Mohammed S. Alqahtani⁵
and Rabbani Syed⁵

1 Department of Chemical Engineering, Qatar University, Doha, Qatar

2 Department of Chemistry, Bilkent University, Bilkent, Ankara, Turkey

3 Department of Biological Sciences and Bioengineering, Indian Institute of
Technology Kanpur, Kanpur, India

4 Department of Chemistry, Rutgers-The State University of New Jersey,
New Brunswick, USA

5 Department of Pharmaceutics, College of Pharmacy, King Saud University,
Riyadh, Saudi Arabia

*Address all correspondence to: roshanandrabi@gmail.com

IntechOpen

© 2021 The Author(s). Licensee IntechOpen. This chapter is distributed under the terms of the Creative Commons Attribution License (<http://creativecommons.org/licenses/by/3.0>), which permits unrestricted use, distribution, and reproduction in any medium, provided the original work is properly cited. 

References

- [1] Nazir R, Kumar A, Ali S, Saad MAS, Al-Marri MJ. Galvanic exchange as a novel method for carbon nitride supported coag catalyst synthesis for oxygen reduction and carbon dioxide conversion. *Catalysts*. 2019;9(10):860.
- [2] Nazir R, Kumar A, Saad MAS, Ashok A. Synthesis of hydroxide nanoparticles of Co/Cu on carbon nitride surface via galvanic exchange method for electrocatalytic CO₂ reduction into formate. *Colloids and Surfaces A: Physicochemical and Engineering Aspects*. 2020; 598:124835.
- [3] Nazir R, Kumar A, Saad MAS, Ali S. Development of CuAg/Cu₂O nanoparticles on carbon nitride surface for methanol oxidation and selective conversion of carbon dioxide into formate. *Journal of Colloid and Interface Science*. 2020; 578:726-737
- [4] Nazir R, Basak U, Pande S. Synthesis of one-dimensional RuO₂ nanorod for hydrogen and oxygen evolution reaction: An efficient and stable electrocatalyst. *Colloids and Surfaces A: Physicochemical and Engineering Aspects*. 2019;560:141-8.
- [5] Ma S, Kenis PJ. Electrochemical conversion of CO₂ to useful chemicals: current status, remaining challenges, and future opportunities. *Current Opinion in Chemical Engineering*. 2013;2(2):191-9.
- [6] Bushuyev OS, De Luna P, Dinh CT, et al. What should we make with CO₂ and how can we make it? *Joule*. 2018;2(5):825-32.
- [7] Yaashikaa P, Kumar PS, Varjani SJ, Saravanan A. A review on photochemical, biochemical and electrochemical transformation of CO₂ into value-added products. *Journal of CO₂ Utilization*. 2019;33:131-47.
- [8] Lu Y, Jiang Z-y, Xu S-w, Wu H. Efficient conversion of CO₂ to formic acid by formate dehydrogenase immobilized in a novel alginate-silica hybrid gel. *Catalysis Today*. 2006;115(1-4):263-8.
- [9] Kalyanasundaram K, Graetzel M. Artificial photosynthesis: biomimetic approaches to solar energy conversion and storage. *Current opinion in Biotechnology*. 2010;21(3):298-310.
- [10] Jouny M, Luc W, Jiao F. General techno-economic analysis of CO₂ electrolysis systems. *Industrial & Engineering Chemistry Research*. 2018;57(6):2165-77.
- [11] Sun Z, Ma T, Tao H, Fan Q, Han B. Fundamentals and challenges of electrochemical CO₂ reduction using two-dimensional materials. *Chem*. 2017;3(4):560-87.
- [12] Cargnello M. Colloidal Nanocrystals as Building Blocks for Well-Defined Heterogeneous Catalysts. *Chemistry of Materials*. 2019;31(3):576-96.
- [13] Wang L, Chen W, Zhang D, et al. Surface strategies for catalytic CO₂ reduction: from two-dimensional materials to nanoclusters to single atoms. *Chemical Society Reviews*. 2019;48(21):5310-49.
- [14] Yin Y, Alivisatos AP. Colloidal nanocrystal synthesis and the organic-inorganic interface. *Nature*. 2005;437(7059):664-70.
- [15] Tang Y, Zheng G. Colloidal nanocrystals for electrochemical reduction reactions. *Journal of colloid and interface science*. 2017;485:308-27.
- [16] Ji X, Song X, Li J, Bai Y, Yang W, Peng X. Size control of gold nanocrystals in citrate reduction: the third role of citrate. *Journal of*

the American Chemical Society.
2007;129(45):13939-48.

[17] Kriegel I, Rodriguez-Fernandez J, Wisnet A, et al. Shedding light on vacancy-doped copper chalcogenides: shape-controlled synthesis, optical properties, and modeling of copper telluride nanocrystals with near-infrared plasmon resonances. *ACS nano*. 2013;7(5):4367-77.

[18] Puntès VF, Krishnan KM, Alivisatos AP. Colloidal nanocrystal shape and size control: the case of cobalt. *Science*. 2001;291(5511):2115-7.

[19] Shevchenko EV, Talapin DV, Schnablegger H, et al. Study of nucleation and growth in the organometallic synthesis of magnetic alloy nanocrystals: the role of nucleation rate in size control of CoPt₃ nanocrystals. *Journal of the American Chemical Society*. 2003;125(30):9090-101.

[20] Alivisatos AP, Gu W, Larabell C. Quantum dots as cellular probes. *Annu. Rev. Biomed. Eng.* 2005;7:55-76.

[21] Heydari N, Ghorashi SMB, Han W, Park H-H. Quantum Dot-Based Light Emitting Diodes (QDLEDs): New Progress. *Quantum-dot Based Light-emitting Diodes*. 2017:25.

[22] Sugimoto T. Preparation of monodispersed colloidal particles. *Advances in Colloid and Interface Science*. 1987;28:65-108.

[23] LaMer VK, Dinegar RH. Theory, production and mechanism of formation of monodispersed hydrosols. *Journal of the American Chemical Society*. 1950;72(11):4847-54.

[24] Vreeland EC, Watt J, Schober GB, et al. Enhanced nanoparticle size control by extending LaMer's mechanism. *Chemistry of Materials*. 2015;27(17):6059-66.

[25] Polte J. Fundamental growth principles of colloidal metal nanoparticles—a new perspective. *CrystEngComm*. 2015;17(36):6809-30.

[26] Murray C, Norris DJ, Bawendi MG. Synthesis and characterization of nearly monodisperse CdE (E = sulfur, selenium, tellurium) semiconductor nanocrystallites. *Journal of the American Chemical Society*. 1993;115(19):8706-15.

[27] Sinatra L, Pan J, Bakr OM. Methods of synthesizing monodisperse colloidal quantum dots. *Material Matters*. 2017;12:3-7.

[28] Kwon SG, Hyeon T. Formation mechanisms of uniform nanocrystals via hot-injection and heat-up methods. *Small*. 2011;7(19):2685-702.

[29] Xia Y, Gilroy KD, Peng HC, Xia X. Seed-mediated growth of colloidal metal nanocrystals. *Angewandte Chemie International Edition*. 2017;56(1):60-95.

[30] Jana NR, Gearheart L, Murphy CJ. Seed-mediated growth approach for shape-controlled synthesis of spheroidal and rod-like gold nanoparticles using a surfactant template. *Advanced Materials*. 2001;13(18):1389-93.

[31] Xia Y, Xiong Y, Lim B, Skrabalak SE. Shape-controlled synthesis of metal nanocrystals: simple chemistry meets complex physics? *Angewandte Chemie International Edition*. 2009;48(1):60-103.

[32] Xia Y, Xia X, Peng H-C. Shape-controlled synthesis of colloidal metal nanocrystals: thermodynamic versus kinetic products. *Journal of the American Chemical Society*. 2015;137(25):7947-66.

[33] Yang TH, Shi Y, Janssen A, Xia Y. Surface Capping Agents and Their Roles in Shape-Controlled Synthesis

of Colloidal Metal Nanocrystals.
Angewandte Chemie International
Edition. 2020;59(36):15378-401.

[34] Verma S, Kim B, Jhong HRM, Ma S, Kenis PJ. A gross-margin model for defining techno-economic benchmarks in the electroreduction of CO₂. *ChemSusChem*. 2016;9(15):1972-9.

[35] Hori Y, Wakebe H, Tsukamoto T, Koga O. Electrocatalytic process of CO selectivity in electrochemical reduction of CO₂ at metal electrodes in aqueous media. *Electrochimica Acta*. 1994;39(11-12):1833-9.

[36] Schouten K, Kwon Y, Van der Ham C, Qin Z, Koper M. A new mechanism for the selectivity to C₁ and C₂ species in the electrochemical reduction of carbon dioxide on copper electrodes. *Chemical Science*. 2011;2(10):1902-9.

[37] Qin B, Wang H, Peng F, Yu H, Cao Y. Effect of the surface roughness of copper substrate on three-dimensional tin electrode for electrochemical reduction of CO₂ into HCOOH. *Journal of CO₂ Utilization*. 2017;21:219-23.

[38] Jiang K, Huang Y, Zeng G, Toma FM, Goddard III WA, Bell AT. Effects of Surface Roughness on the Electrochemical Reduction of CO₂ over Cu. *ACS Energy Letters*. 2020;5(4):1206-14.

[39] Kuhl KP, Cave ER, Abram DN, Jaramillo TF. New insights into the electrochemical reduction of carbon dioxide on metallic copper surfaces. *Energy & Environmental Science*. 2012;5(5):7050-9.

[40] Fan L, Xia C, Yang F, Wang J, Wang H, Lu Y. Strategies in catalysts and electrolyzer design for electrochemical CO₂ reduction toward C₂+ products. *Science Advances*. 2020;6(8):eaay3111.

[41] Kleis J, Greeley J, Romero N, et al. Finite size effects in chemical bonding:

From small clusters to solids. *Catalysis Letters*. 2011;141(8):1067-71.

[42] Huang J, Buonsanti R. Colloidal nanocrystals as heterogeneous catalysts for electrochemical CO₂ conversion. *Chemistry of Materials*. 2018;31(1):13-25.

[43] Liu S, Huang S. Size effects and active sites of Cu nanoparticle catalysts for CO₂ electroreduction. *Applied Surface Science*. 2019;475:20-7.

[44] Kim D, Resasco J, Yu Y, Asiri AM, Yang P. Synergistic geometric and electronic effects for electrochemical reduction of carbon dioxide using gold-copper bimetallic nanoparticles. *Nature communications*. 2014;5(1):1-8.

[45] Sneed BT, Young AP, Tsung C-K. Building up strain in colloidal metal nanoparticle catalysts. *Nanoscale*. 2015;7(29):12248-65.

[46] Loiudice A, Lobaccaro P, Kamali EA, et al. Tailoring copper nanocrystals towards C₂ products in electrochemical CO₂ reduction. *Angewandte Chemie International Edition*. 2016;55(19):5789-92.

[47] Zhu W, Michalsky R, Metin On, et al. Monodisperse Au nanoparticles for selective electrocatalytic reduction of CO₂ to CO. *Journal of the American Chemical Society*. 2013;135(45):16833-6.

[48] Suen N-T, Kong Z-R, Hsu C-S, et al. Morphology manipulation of copper nanocrystals and product selectivity in the electrocatalytic reduction of carbon dioxide. *ACS Catalysis*. 2019;9(6):5217-22.

[49] Zhou Z-Y, Tian N, Huang Z-Z, Chen D-J, Sun S-G. Nanoparticle catalysts with high energy surfaces and enhanced activity synthesized by electrochemical method. *Faraday discussions*. 2009;140:81-92.

- [50] Lee H-E, Yang KD, Yoon SM, et al. Concave rhombic dodecahedral Au nanocatalyst with multiple high-index facets for CO₂ reduction. *ACS nano*. 2015;9(8):8384-93.
- [51] Nørskov JK, Bligaard T, Rossmeisl J, Christensen CH. Towards the computational design of solid catalysts. *Nature chemistry*. 2009;1(1):37-46.
- [52] Huang H, Jia H, Liu Z, et al. Understanding of strain effects in the electrochemical reduction of CO₂: using Pd nanostructures as an ideal platform. *Angewandte Chemie*. 2017;129(13):3648-52.
- [53] Kortlever R, Peters I, Koper S, Koper MT. Electrochemical CO₂ reduction to formic acid at low overpotential and with high faradaic efficiency on carbon-supported bimetallic Pd–Pt nanoparticles. *Acs Catalysis*. 2015;5(7):3916-23.
- [54] Kwon IS, Debela TT, Kwak IH, et al. Selective electrochemical reduction of carbon dioxide to formic acid using indium–zinc bimetallic nanocrystals. *Journal of Materials Chemistry A*. 2019;7(40):22879-83.
- [55] Guo X, Zhang Y, Deng C, et al. Composition dependent activity of Cu–Pt nanocrystals for electrochemical reduction of CO₂. *Chemical Communications*. 2015;51(7):1345-8.
- [56] Kim M-G, Jeong J, Choi Y, et al. Synthesis of V-doped In₂O₃ Nanocrystals via Digestive-Ripening Process and Their Electrocatalytic Properties in CO₂ Reduction Reaction. *ACS Applied Materials & Interfaces*. 2020;12(10):11890-7.
- [57] Al-Omari AA, Yamani ZH, Nguyen HL. Electrocatalytic CO₂ reduction: from homogeneous catalysts to heterogeneous-based reticular chemistry. *Molecules*. 2018;23(11):2835.
- [58] Xiang W, Zhang Y, Lin H, Liu C-j. Nanoparticle/metal–organic framework composites for catalytic applications: current status and perspective. *Molecules*. 2017;22(12):2103.
- [59] Guntern YT, Pankhurst JR, Vávra J, et al. Nanocrystal/Metal–Organic Framework Hybrids as Electrocatalytic Platforms for CO₂ Conversion. *Angewandte Chemie International Edition*. 2019;58(36):12632-9.
- [60] Wang Z, Wu L, Sun K, et al. Surface Ligand Promotion of Carbon Dioxide Reduction through Stabilizing Chemisorbed Reactive Intermediates. *The journal of physical chemistry letters*. 2018;9(11):3057-61.
- [61] Zhao Y, Fu G, Zheng N. Shaping the selectivity in heterogeneous hydrogenation by using molecular modification strategies: Experiment and theory. *Catalysis Today*. 2017;279:36-44.
- [62] Liu P, Qin R, Fu G, Zheng N. Surface coordination chemistry of metal nanomaterials. *Journal of the American Chemical Society*. 2017;139(6):2122-31.
- [63] Pankhurst JR, Guntern YT, Mensi M, Buonsanti R. Molecular tunability of surface-functionalized metal nanocrystals for selective electrochemical CO₂ reduction. *Chemical science*. 2019;10(44):10356-65.
- [64] Cao Z, Kim D, Hong D, et al. A molecular surface functionalization approach to tuning nanoparticle electrocatalysts for carbon dioxide reduction. *Journal of the American Chemical Society*. 2016;138(26):8120-5.
- [65] Fujishima A, Honda K. Electrochemical photolysis of water at a semiconductor electrode. *nature*. 1972;238(5358):37-8.
- [66] Khaselev O, Turner JA. A monolithic photovoltaic-photoelectrochemical

device for hydrogen production via water splitting. *Science*. 1998;280(5362):425-7.

[67] Paracchino A, Laporte V, Sivula K, Grätzel M, Thimsen E. Highly active oxide photocathode for photoelectrochemical water reduction. *Nature materials*. 2011;10(6):456-61.

[68] Zhu J, Hu L, Zhao P, Lee LYS, Wong K-Y. Recent advances in electrocatalytic hydrogen evolution using nanoparticles. *Chemical Reviews*. 2019;120(2):851-918.

[69] Das RK, Wang Y, Vasilyeva SV, et al. Extraordinary hydrogen evolution and oxidation reaction activity from carbon nanotubes and graphitic carbons. *ACS Nano*. 2014;8(8):8447-56.

[70] Kibler LA. Hydrogen electrocatalysis. *ChemPhysChem*. 2006;7(5):985-91.

[71] Greeley J, Markovic NM. The road from animal electricity to green energy: combining experiment and theory in electrocatalysis. *Energy & Environmental Science*. 2012;5(11):9246-56.

[72] Conway B, Tilak B. Interfacial processes involving electrocatalytic evolution and oxidation of H₂, and the role of chemisorbed H. *Electrochimica Acta*. 2002;47(22-23):3571-94.

[73] Walter MG, Warren EL, McKone JR, et al. Solar water splitting cells. *Chemical reviews*. 2010;110(11):6446-73.

[74] Zheng Y, Jiao Y, Zhu Y, et al. Hydrogen evolution by a metal-free electrocatalyst. *Nature communications*. 2014;5(1):1-8.

[75] Feng Y, Yu X-Y, Paik U. Nickel cobalt phosphides quasi-hollow nanocubes as an efficient electrocatalyst for hydrogen evolution in alkaline solution. *Chemical Communications*. 2016;52(8):1633-6.

[76] Korzeniewski C, Wieckowski A, Norskov J. Vibrational spectroscopy for the characterization of pem fuel cell membrane materials. *Fuel Cell Science: Theory, Fundamentals, and Biocatalysis*. 2010:395-413.

[77] Shinagawa T, Garcia-Esparza AT, Takanabe K. Insight on Tafel slopes from a microkinetic analysis of aqueous electrocatalysis for energy conversion. *Scientific reports*. 2015;5:13801.

[78] Ouyang Y, Ling C, Chen Q, Wang Z, Shi L, Wang J. Activating inert basal planes of MoS₂ for hydrogen evolution reaction through the formation of different intrinsic defects. *Chemistry of Materials*. 2016;28(12):4390-6.

[79] Sabatier P. *Le catalyse en chimie organique* Berange. Paris; 1920.

[80] Marković N, Ross Jr P. Surface science studies of model fuel cell electrocatalysts. *Surface Science Reports*. 2002;45(4-6):117-229.

[81] Nørskov JK, Bligaard T, Logadottir A, et al. Trends in the exchange current for hydrogen evolution. *Journal of The Electrochemical Society*. 2005;152(3):J23.

[82] Parsons R. Volcano curves in electrochemistry. *Catalysis in Electrochemistry*. 2011:1-15.

[83] Conway B, Jerkiewicz G. Relation of energies and coverages of underpotential and overpotential deposited H at Pt and other metals to the 'volcano curve' for cathodic H₂ evolution kinetics. *Electrochimica Acta*. 2000;45(25-26):4075-83.

[84] Sarkar S, Peter SC. An overview on Pd-based electrocatalysts for the hydrogen evolution reaction. *Inorganic Chemistry Frontiers*. 2018;5(9):2060-80.

[85] Huang Y-X, Liu X-W, Sun X-F, et al. A new cathodic electrode deposit

with palladium nanoparticles for cost-effective hydrogen production in a microbial electrolysis cell. *International Journal of Hydrogen Energy*. 2011;36(4):2773-6.

[86] Joshi U, Malkhandi S, Ren Y, Tan TL, Chiam SY, Yeo BS. Ruthenium-Tungsten Composite Catalyst for the Efficient and Contamination-Resistant Electrochemical Evolution of Hydrogen. *ACS Applied Materials & Interfaces*. 2018;10(7):6354-60.

[87] Li F, Han GF, Noh HJ, Ahmad I, Jeon IY, Baek JB. Mechanochemically assisted synthesis of a Ru catalyst for hydrogen evolution with performance superior to Pt in both acidic and alkaline media. *Advanced Materials*. 2018;30(44):1803676.

[88] Miles M, Thomason M. Periodic variations of overvoltages for water electrolysis in acid solutions from cyclic voltammetric studies. *Journal of the Electrochemical Society*. 1976;123(10):1459.

[89] Xu YF, Gao MR, Zheng YR, Jiang J, Yu SH. Nickel/nickel (II) oxide nanoparticles anchored onto cobalt (IV) diselenide nanobelts for the electrochemical production of hydrogen. *Angewandte Chemie*. 2013;125(33):8708-12.

[90] Qiu HJ, Ito Y, Cong W, et al. Nanoporous graphene with single-atom nickel dopants: an efficient and stable catalyst for electrochemical hydrogen production. *Angewandte Chemie International Edition*. 2015;54(47):14031-5.

[91] Zou X, Huang X, Goswami A, et al. Cobalt-embedded nitrogen-rich carbon nanotubes efficiently catalyze hydrogen evolution reaction at all pH values. *Angewandte Chemie*. 2014;126(17):4461-5.

[92] Zhang L, Zhu S, Dong S, et al. Co nanoparticles encapsulated in

porous N-doped carbon nanofibers as an efficient electrocatalyst for hydrogen evolution reaction. *Journal of The Electrochemical Society*. 2018;165(15):J3271.

[93] Eyert V, Horny R, Höck K-H, Horn S. Embedded Peierls instability and the electronic structure of MoO₂. *Journal of Physics: Condensed Matter*. 2000;12(23):4923.

[94] Tang YJ, Gao MR, Liu CH, et al. Porous molybdenum-based hybrid catalysts for highly efficient hydrogen evolution. *Angewandte Chemie*. 2015;127(44):13120-4.

[95] Jing S, Lu J, Yu G, et al. Carbon-encapsulated WO_x hybrids as efficient catalysts for hydrogen evolution. *Advanced Materials*. 2018;30(28):1705979.

[96] Ham DJ, Lee JS. Transition metal carbides and nitrides as electrode materials for low temperature fuel cells. *Energies*. 2009;2(4):873-99.

[97] Zhu Y, Chen G, Xu X, Yang G, Liu M, Shao Z. Enhancing electrocatalytic activity for hydrogen evolution by strongly coupled molybdenum nitride@ nitrogen-doped carbon porous nano-octahedrons. *ACS Catalysis*. 2017;7(5):3540-7.

[98] Zhu Y, Chen G, Zhong Y, Zhou W, Shao Z. Rationally Designed Hierarchically Structured Tungsten Nitride and Nitrogen-Rich Graphene-Like Carbon Nanocomposite as Efficient Hydrogen Evolution Electrocatalyst. *Advanced Science*. 2018;5(2):1700603.

[99] Lv H, Chen X, Xu D, et al. Ultrathin PdPt bimetallic nanowires with enhanced electrocatalytic performance for hydrogen evolution reaction. *Applied Catalysis B: Environmental*. 2018;238:525-32.

[100] Yang T, Zhu H, Wan M, Dong L, Zhang M, Du M. Highly efficient and

durable PtCo alloy nanoparticles encapsulated in carbon nanofibers for electrochemical hydrogen generation. *Chemical Communications*. 2016;52(5):990-3.

[101] Quaino P, Santos E, Wolfschmidt H, Montero M, Stimming U. Theory meets experiment: electrocatalysis of hydrogen oxidation/evolution at Pd–Au nanostructures. *Catalysis today*. 2011;177(1):55-63.

[102] Chen J, Xia G, Jiang P, et al. Active and durable hydrogen evolution reaction catalyst derived from Pd-doped metal–organic frameworks. *ACS Applied Materials & Interfaces*. 2016;8(21):13378-83.

[103] Su J, Yang Y, Xia G, Chen J, Jiang P, Chen Q. Ruthenium-cobalt nanoalloys encapsulated in nitrogen-doped graphene as active electrocatalysts for producing hydrogen in alkaline media. *Nature communications*. 2017;8(1):1-12.

[104] Zhang C, Liu Y, Chang Y, et al. Component-controlled synthesis of necklace-like hollow Ni_xRu_y nanoalloys as electrocatalysts for hydrogen evolution reaction. *ACS Applied Materials & Interfaces*. 2017;9(20):17326-36.

[105] Zhang J, Wang T, Liu P, et al. Efficient hydrogen production on MoNi₄ electrocatalysts with fast water dissociation kinetics. *Nature communications*. 2017;8(1):1-8.

[106] Chen J, Ge Y, Feng Q, et al. Nesting Co₃Mo binary alloy nanoparticles onto molybdenum oxide nanosheet arrays for superior hydrogen evolution reaction. *ACS applied materials & interfaces*. 2019;11(9):9002-10.

[107] Chen J, Yang Y, Su J, Jiang P, Xia G, Chen Q. Enhanced activity for hydrogen evolution reaction over CoFe catalysts by alloying with small amount of Pt. *ACS applied materials & interfaces*. 2017;9(4):3596-601.